Temporal characteristics of high band-pass filtered teleseismic P-waveforms from large shallow earthquakes

Tatsuhiko Hara

International Institute of Seismology and Earthquake Engineering, Building Research Institute, 1 Tatehara, Tsukuba, Ibaraki 305-0802, Japan

(Received September 21, 2007; Revised March 10, 2008; Accepted March 25, 2008; Online published August 4, 2008)

We measured time differences between P-wave arrivals and the times at which squared amplitudes of high bandpass (2–4 Hz) filtered P-waves became the largest for large shallow earthquakes that occurred during the period 1995–2007. The time differences were then normalized by twice the centroid time shift for the corresponding earthquakes. We found that most of the seismograms had normalized time differences that congregated at about 50% (corresponding to centroid time shifts). Few normalized time differences were found in the 0–20% range. These results support the use of this time difference to infer the order of the source duration and, thereby, the effectiveness of the duration measurement procedure of the high-frequency energy radiation that we recently developed.

Key words: High-frequency energy radiation, shallow earthquake.

1. Introduction

It is important to be able to rapidly determine earthquake magnitudes in order to issue tsunami early warnings. The results of studies carried out since the occurrence of the devastating Sumatra earthquake on December 26, 2004 suggest that durations of P-wave high-frequency energy radiation can be utilized to quantify the sizes of earthquakes (e.g., Lomax, 2005; Lomax and Michelini, 2005; Ni *et al.*, 2005; Park *et al.*, 2005; Chen *et al.*, 2006; Lomax *et al.*, 2007). We have recently developed a method to determine earthquake magnitudes using durations of P-wave high-frequency energy radiation and maximum displacement amplitudes (Hara, 2007a). We have also shown that this method is applicable to tsunami earthquakes (Hara, 2007b).

In this method, we measure the difference between P-wave arrival time and the time when the squared amplitude of a band-pass filtered time-series becomes the largest and use this difference to infer the order of the source duration. This time difference is used to determine the appropriate length of a time window for smoothing the time-series to allow a better determination of the duration of high-frequency energy radiation from seismograms. Hara (2007a) showed that this procedure was applicable to large earthquakes, including the December 26, 2004 Sumatra earthquake. In the study reported here, we investigated the distribution of this time difference, which hereafter we call the peak time, and discuss the effectiveness of our smoothing procedure.

2. Data

The selection criteria for earthquakes to be analyzed in this study were: (1) the earthquake occurred between 1995 and September 2007; (2) the focal depth was shallow ($\leq$50 km); (3) the moment magnitude in the Global CMT catalog (http://www.globalcmt.org/) is $\geq$7.2; (4) the centroid time shift (i.e., difference between the origin time and centroid times) is $\geq$10 s. We adopted the fourth condition taking the larger effect of the coda wave for a shorter source time into consideration (e.g., Ritter *et al.*, 1997). Hara (2007a) showed that for the November 3, 2002 Denali earthquake, his measurement procedure extracted only the initial thrust subevent, the high-frequency energy radiation duration of which was about 17 s. Therefore, we did not include this event in the dataset. A total of 68 earthquakes were selected. We retrieved BHZ channel waveform data of the Global Seismograph Network (GSN) stations for these earthquakes from IRIS DMC. Following Ni *et al.* (2005), we used data from stations within the epicentral distance range of 30–85° to avoid scattering due to the upper mantle or D$''$ structures (Shearer and Earle, 2004).

3. Measurement Procedure

We measured peak times (defined above as differences between P-wave arrival times and times when the amplitudes of the band-pass filtered P-waves become the largest) as follows. The steps of this measurement procedure are the same as the first five steps used by Hara (2007a). After the baseline correction was carried out, we applied the band-pass filter with corner frequencies of 2 and 4 Hz. We then squared each data point of the time-series. We picked P-wave arrivals using a STA/LTA approach, where the duration for STA was 0.2 s, that for LTA was 10 s, and the threshold value of the ratio STA/LTA for P-wave detection was 25. After this automatic picking was carried out, we checked observed seismograms and processed time series; then, if necessary, we corrected P-wave arrivals. We discarded noisy data in this step. Finally, we found the peak of the time-series from the arrival of P-waves within a given

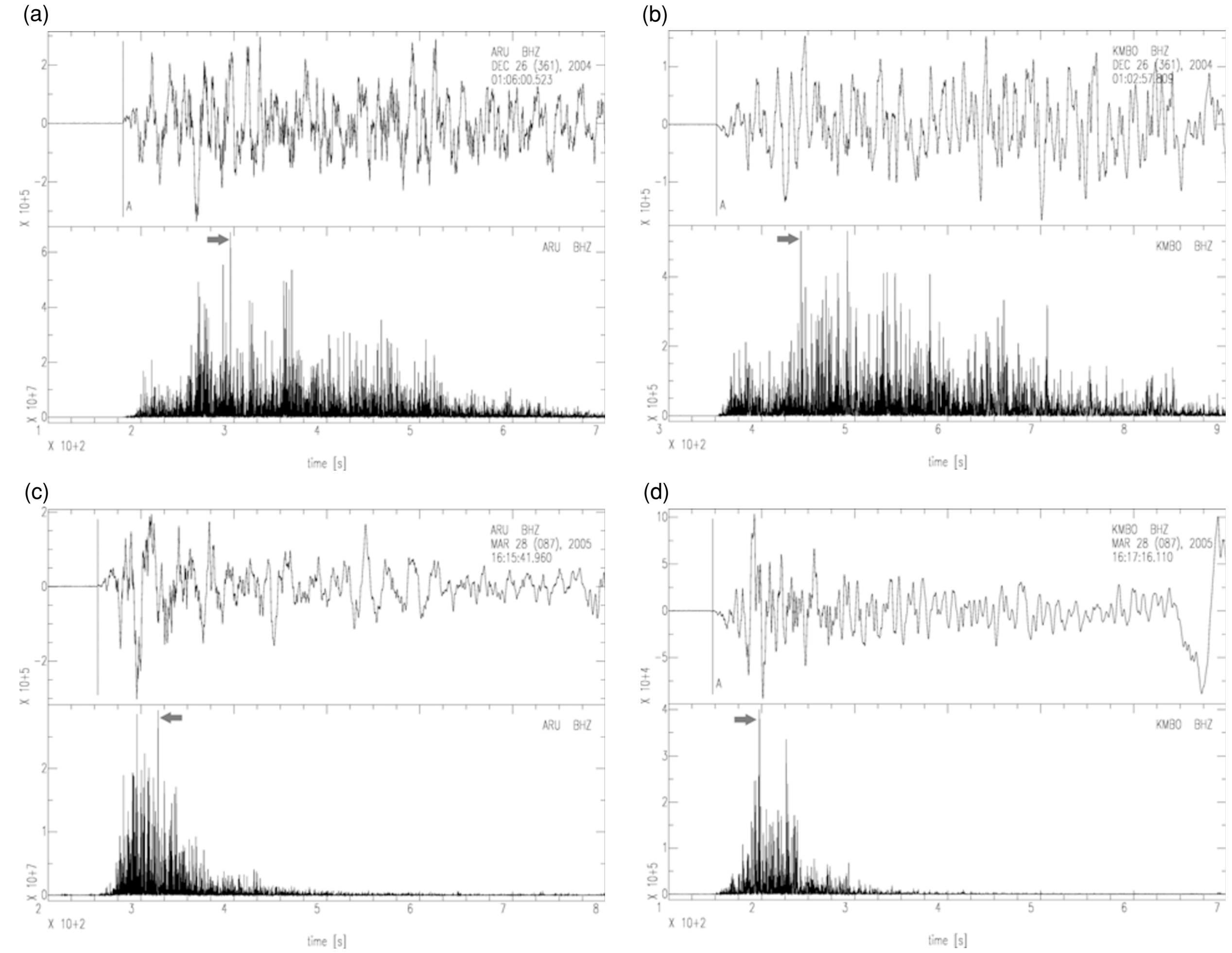

Fig. 1. Examples of measurements of peak times for the December 26, 2004 Sumatra (a, b) and the March 28, 2005 Northern Sumatra (c, d) earthquakes. The upper and lower traces in each figure are an observed seismogram and a time series of squares of band-pass (2–4 Hz) filtered seismogram, respectively. The arrows in the lower panels show the peaks for which the peak times are measured.

time window (400 s) and calculated the corresponding peak time. Figure 1 shows examples of measurements of peak times for the December 26, 2004 Sumatra ($M_w = 9.0$) and the March 28, 2005 Northern Sumatra ($M_w = 8.6$) earthquakes.

4. Results

Figure 2(a) shows all of the measured peak times as a function of centroid time shifts (i.e., differences between origin times and centroid times), which are likely to correlate with source times. There is a tendency that peak times increase as centroid time shifts increase, which is not surprising considering the longer source durations. There is also a tendency—with a few exceptions—that the shortest duration for a certain earthquake increases as the centroid time shifts increase. For the case of the 2004 December 26 Sumatra earthquake, the shortest peak time is 39.1 s. In order to investigate relation between peak times and source durations, we normalized the measured peak times by twice the centroid time shifts, which are rough guesses of source times (Fig. 2(b)). There are few data points in earlier parts (say, 0–20% of the vertical scale), while the observations concentrate around 50%, which corresponds to the centroid time shifts.

In order to observe the distribution of the normalized peak times more clearly, the frequencies of the peak times are shown in Fig. 3 for three cases: (1) only events whose centroid time shifts are less than 20 s; (2) only events whose centroid time shifts are ≥20 s and <40 s; (3) only events whose centroid time shifts are ≥40 s. The frequency distributions for these three cases are similar to each other, although the tail in case (1) is longer, which is likely to be due to the larger effect of coda waves for shorter source durations. The common features among these three cases are the low frequency in the range of 0–20% and the high frequency around 50%. Therefore, if we use peak times to obtain a rough guess for the source time of a certain earthquake with data from a few tens of stations, the approach will work well in most cases owing to these characteristics. This is the reason why the smoothing procedure of Hara (2007a) worked well, where one-sixth of peak times were used as the width of moving window average.

5. Discussion

We have shown that only a small percentage of the seismograms had normalized peak times in the range 0–20% and that most of the seismograms had normalized peak times near 50% or about the centroid time shift. Figure 4

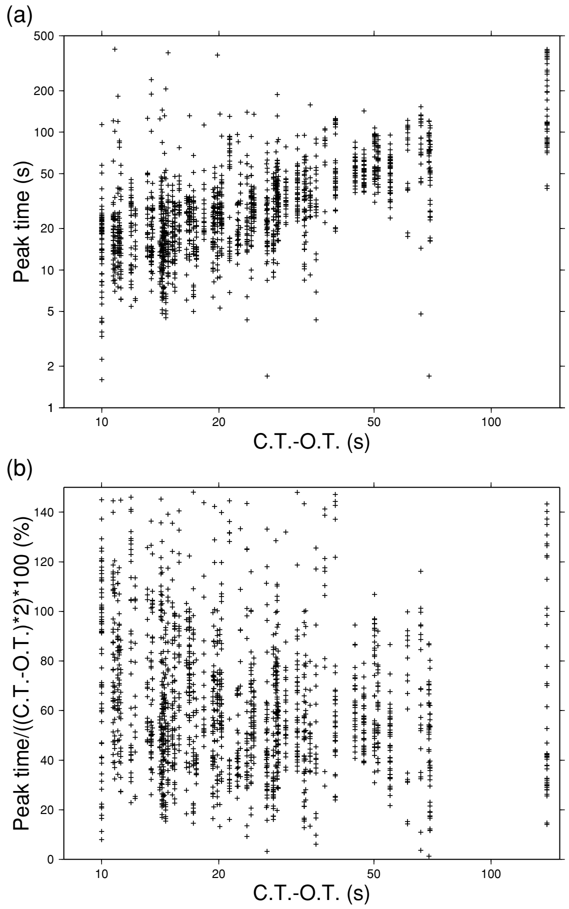

Fig. 2. (a) The measured peak times as a function of centroid time shifts. (b) The peak times normalized by twice of centroid time shifts as a function of centroid time shifts.

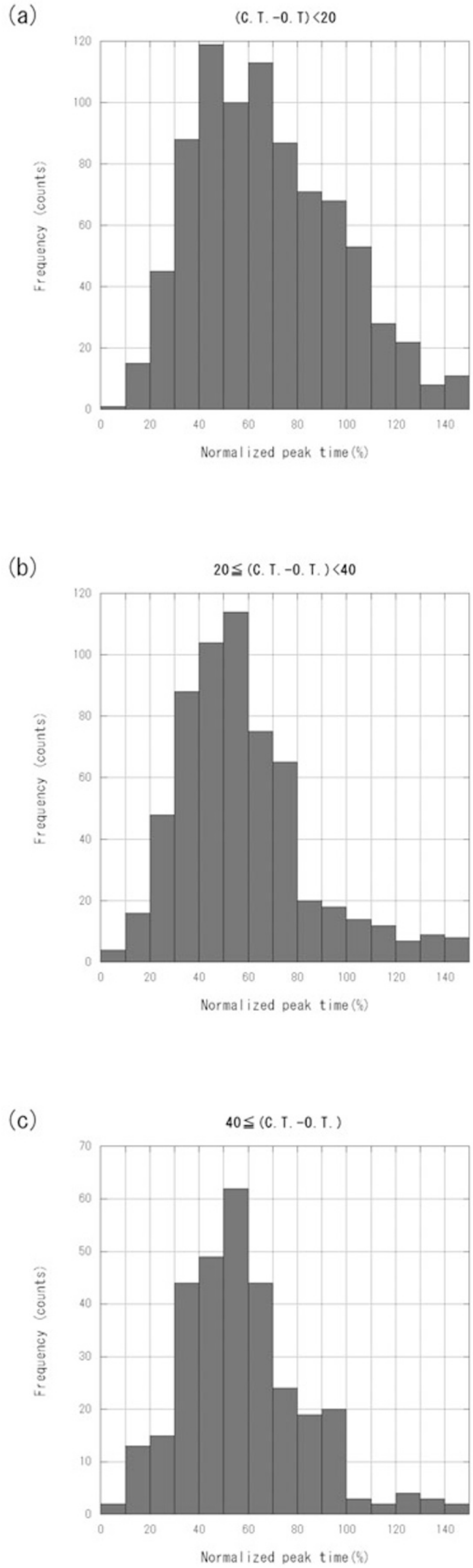

Fig. 3. The frequencies of the normalized peak times from only events whose centroid time shifts are less than 20 s (a), only events whose centroid time shifts are ≥20 s and <40 s (b), and only events whose centroid time shifts are ≥40 s (c).

shows the frequency of the mean normalized peak times calculated for each earthquake. There is no earthquake for which a mean normalized peak time is in the range of 0–30%. Therefore, if we use this mean, it may be possible to reduce the probability to underestimate the duration of high-frequency energy radiation, although it will take a longer time to determine magnitudes.

There are four events for which the mean normalized peak times exceed 100%: the 1998 March 25 Antarctic, 2002 March 5, 2002 October 10, and 2005 July 24 earthquakes. For the 1998 March 25 Antarctic earthquake, the results of some studies suggest that this earthquake consisted of two large subevents (e.g., Henry *et al.*, 2000), and it is likely that the measured peak time corresponds to the second subevent. For these events, the measured durations of high-frequency energy radiation are in the range of 167–218% of twice the centroid time shifts, which may lead to possible errors of magnitude estimates up to 0.23 following the magnitude formula of Hara (2007a). The actual differences between the moment magnitudes of the Global CMT catalog and the magnitudes obtained by the procedure of Hara (2007a) are within 0.15 for these events. Therefore, we find no serious problems in determining the magnitudes of these earthquakes, although it is desirable to improve our duration measurement procedure for these cases.

Figure 4(b) and (c) show the frequencies of the mean normalized peak times for the thrust events and those for the strike slip events. We followed Frohlich and Apperson (1992) to classify focal mechanisms. Since there are only two normal fault events in our dataset, we did not show their

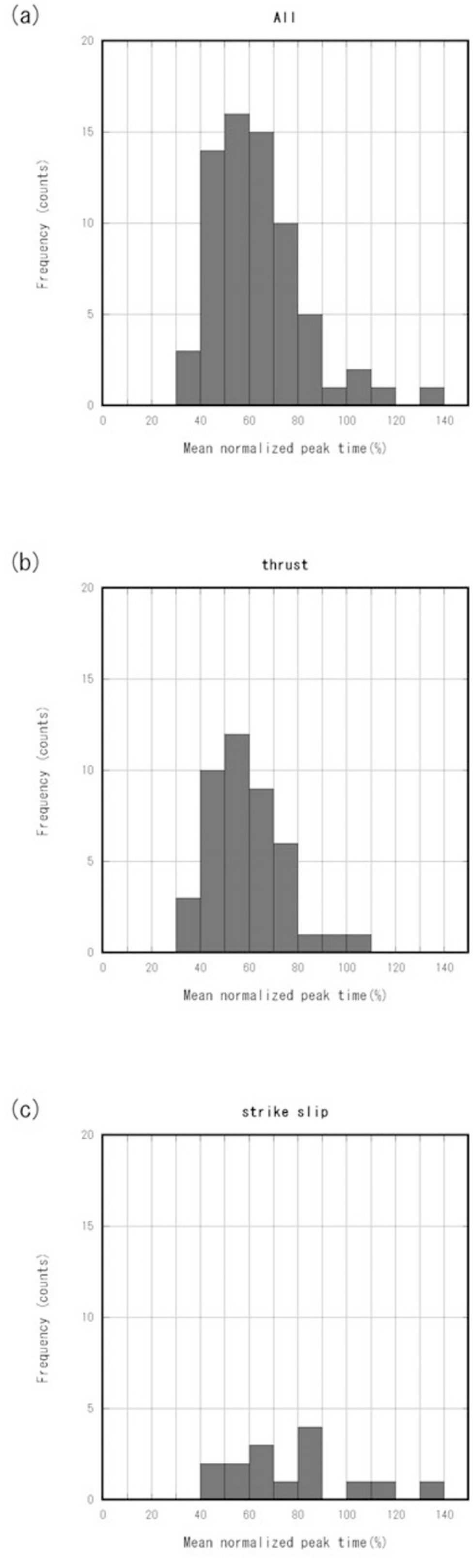

Fig. 4. The frequencies of the mean normalized peak times for all of the events, thrust events, and strike slip events are shown in (a), (b) and (c), respectively.

frequency. It seems that there is a tendency for the mean normalized peak times for strike slip events to be larger that those for thrust events. However, it is difficult to draw a definite conclusion given that the number of strike slip events is much smaller than that of the thrust events in our dataset.

The frequencies shown in Figs. 3 and 4 imply that the high-frequency energy radiation is weak in the vicinity of rupture starting regions. The systematic determination of spatial and temporal distributions of high-frequency energy radiation for a set of earthquakes considering seismic wave propagation and site effects using techniques such as the empirical Green's function method (e.g., Gusev *et al*., 2007) will be an interesting issue to be studied in future research.

Acknowledgments. The author thanks Drs. Taro Okamoto and Naoki Kobayashi for their comments. The author also thanks Dr. Stuart A. Weinstein and the anonymous reviewer for their comments on the earlier version of this paper, which contributed greatly to an improvement in the manuscript. The author thanks Mr. Naoki Nishimura for his permission to use his program to classify focal mechanisms. We used SAC (Seismic Analysis Code) (Goldstein *et al*., 2007) for seismic waveform data analyses in this study. The Generic Mapping Tools software program (GMT, Wessel and Smith, 1998) was used to make the figure.

References

Chen, Y., J. Huang, S. Ni, and Y. Chen, Slow rupture velocity of the July 17th, 2006 Java earthquake from high frequency analysis, *Eos Trans. AGU*, **87**(52), Fall Meet. Suppl., Abstract S21A-0128, 2006.

Frohlich, C. and K. D. Apperson, Earthquake focal mechanisms, moment tensors, and the consistency of seismic activity near plate boundaries, *Tectonics*, **11**, 279–296, 1992.

Goldstein, P., D. Dodge, M. Firpo, L. Minner, J. E. Tull, D. Harris, and W. C. Tapley, SAC—Seismic Analysis Code, http://www.iris.edu/manuals/sac/manual.html, 2007.

Gusev, A. A., E. M. Guseva, and G. F. Panza, Size and duration of the high-frequency radiator in the source of the 2004 December 26 Sumatra earthquake, *Geophys. J. Int.*, **170**, 1119–1128, doi:10.1111/j.1365-246X.2007.03368.x, 2007.

Hara, T., Measurement of the duration of high-frequency energy radiation and its application to determination of the magnitudes of large shallow earthquakes, *Earth Planets Space*, **59**, 227–231, 2007a.

Hara, T., Magnitude determination using duration of high frequency energy radiation and displacement amplitude: application to tsunami earthquakes, *Earth Planets Space*, **59**, 561–565, 2007b.

Henry, C., S. Das, and J. H. Woodhouse, The great March 25, 1998, Antarctic Plate earthquake: Moment tensor and rupture history, *J. Geophys. Res.*, **105**, 16097–16118, 2000.

Lomax, A., Rapid estimation of rupture extent for large earthquakes: Application to the 2004, M9 Sumatra-Andaman mega-thrust, *Geophys. Res. Lett.*, **32**, L10314, doi:10.1029/2005GL022437, 2005.

Lomax, A. and A. Michelini, Rapid determination of earthquake size for hazard warning, *Eos Trans. AGU*, **86**(21), 202, 2005.

Lomax, A., A. Michelini, and A. Piatanesi, An energy-duration procedure for rapid determination of earthquake magnitude and tsunamigenic potential, *Geophys. J. Int.*, **170**, doi:10.1111/j.1365-246X.2007.03469.x, 1195–1209, 2007.

Ni, S., H. Kanamori, and D. Helmberger, Energy radiation from the Sumatra earthquake, *Nature*, **434**, 582, 2005.

Park, J., K. Anderson, R. Aster, R. Butler, T. Lay, and D. Simpson, Global seismographic network records the great Sumatra-Andaman earthquake, *Eos Trans. AGU*, **86**(6), 57, 2005.

Ritter, J. R. R., P. M. Mai, G. Stoll, and K. Fuchs, Scattering of teleseismic waves in the lower crust Observations in the Massif Central, France, *Phys. Earth Planet. Inter.*, **104**, 127–146, 1997.

Shearer, P. M. and P. S. Earle, The global short-period wavefield modelled with a Monte Carlo seismic phonon method, *Geophys. J. Int.*, **158**, 1103–1117, 2004.

Wessel, P. and W. H. F. Smith, New, improved version of the Generic Mapping Tools released, *EOS Trans. AGU*, **79**(47), 579, 1998.

T. Hara (e-mail: thara@kenken.go.jp)